Electronic Research Archive

ERA, 31(1): 342–366.
DOI: 10.3934/era.2023017
Received: 22 August 2022
Revised: 17 October 2022
Accepted: 20 October 2022
Published: 02 November 2022

http://www.aimspress.com/journal/era

Research article

On the driver's stochastic nature in car-following behavior: Modeling and stabilizing based on the V2I environment

Ying Luo[1], Yanyan Chen[1], Kaiming Lu[1], Jian Zhang[1,*], Tao Wang[2] and Zhiyan Yi[3]

[1] Beijing Key Laboratory of Traffic Engineering, Beijing University of Technology, Beijing 100124, China
[2] School of Vehicle and Mobility, Tsinghua University, Beijing 100084, China
[3] Department of Civil & Environmental Engineering, University of Utah, Salt Lake City, UT 84112, United States of America

* **Correspondence:** Email: jian.zhang@bjut.edu.cn.

Abstract: The driver's stochastic nature is one of the important causes of traffic oscillation. To better describe the impact of the driver's stochastic characteristics on car-following behavior, we propose a stochastic full velocity difference model (SFVDM) considering the stochastic variation of the desired velocity. In order to mitigate traffic oscillation caused by driving stochasticity, we further propose a stable speed guidance model (S-SFVDM) by leveraging vehicle-to-infrastructure communication. Stochastic linear stability conditions are derived to demonstrate the prominent influence of the driver's stochasticity on the stability of traffic flow and the improvement of traffic flow stability by the proposed guidance strategy, respectively. We present numerical tests to demonstrate the effectiveness of the proposed models. The results show that the SFVDM can capture the traffic oscillation caused by the driver's stochastic desired velocity and reproduce the same disturbance growth pattern as in the field experiment. The results also indicate that the S-SFVDM can significantly expand the stable area of traffic flow to decrease the negative impact on traffic flow stability caused by the driver's stochastic nature.

Keywords: stochastic car-following model; stochastic stability analysis; V2I environment; stable control

1. Introduction

With the rapid increase of car occupancies, traffic congestion is becoming more and more serious, leading to tremendous environmental pollution and economic losses. Researchers have proposed many traffic flow models to study the mechanism behind complex traffic phenomena and provide a myriad of solutions to solve practical traffic problems. Among them, the car-following model offers an effective way to understand the mechanism of various complex traffic phenomena (such as traffic oscillation) from the perspective of individual interactions at the microscopic level. In 1961, Newell [1] proposed a car-following model that takes the optimal velocity into account and aligned with the experimental data of the steady flow. In 1995, Bando et al. [2] put forward an optimal velocity model (OVM), which successfully reproduced the evolution process for traffic congestion and received significant attention from many researchers later. However, the OVM may generate unrealistic values of acceleration and deceleration. To overcome this problem, Helbing and Tilch [3] proposed a generalized force model (GFM), which has a better fit with field data. GFM only considered the influence of a negative velocity difference on acceleration. In 2001, Jiang et al. [4] proposed the full velocity difference model (FVDM), considering negative and positive velocity differences.

Based on those classical car-following models, many extended models were proposed by considering different factors from various perspectives. Yu and Shi [5] introduced the changes of multiple preceding cars' velocity with memory and formulated a new connected cruise control strategy, improving traffic safety and reducing fuel consumption. Chen et al. [6] proposed an extended OVM by considering multi-anticipative optimal velocity. The vehicle's acceleration was described as a function of the optimal velocity and desired distance to improve traffic flow stability. Based on the FVDM, the driver's backward-looking effect and traffic interruption probability were both integrated into the car-following model at the same time to enhance traffic flow stability effectively [7]. Considering the influence of the driver's memory, Tang et al. [8] and Liu et al. [9] proposed extended car-following models and illustrated that the driver's memory positively affected traffic flow stability. Apart from the above studies, many scholars [10–20] have also enriched the research in this field. Furthermore, the distribution of the driver's memory was considered, making the simulation results of car-following models closer to the empirical results [21,22]. Hossain et al. [23] redefined the backward-looking effect by proposing a positive backward equilibrium speed function based on the perspective of mathematical and physical theories, which strengthened the stability of traffic flow.

With the emergence of advanced technologies, vehicle-to-vehicle (V2V) and vehicle-to-infrastructure (V2I) communication have great potential to mitigate traffic congestion and improve traffic safety. Jia and Ngoduy [24] incorporated V2V and V2I information into the following model and investigated the effects on driver behavior and traffic stability. Xiao et al. [25] proposed an expanded non-lane-based FVDM based on V2V communication technology. Ngoduy [26] studied the stability of heterogeneous traffic flow in a connected environment and derived the string stability conditions of the traffic flow. Larsson et al. [27] proposed a pro-social control strategy for connected autonomous vehicles in a mixed traffic flow environment to mitigate traffic fluctuations caused by human-driven vehicles. Numerous studies [28–34] applied intelligent traffic systems to reduce the instability of traffic flow by incorporating more dynamic traffic information into car-following models. Furthermore, Wu and Qu [35] discussed the positive role of connected technology in improving traffic flow efficiency and reducing energy consumption. Olovsson et al. [36] investigated the communication demands, privacy and network security issues of connected vehicles. In the meantime, the construction

of the commercial data platform and infrastructure of connected vehicles has also been advancing [37].

Up to now, studies on deterministic car-following models have made tremendous achievements. Yet, the deterministic car-following models cannot delineate the uncertainty of the driver's perception and behavior [38]. In fact, the driver's stochastic nature is one of the important causes of traffic oscillation. Previous experiments [38–44] indicated that standard deviations of the velocity increase in a concave way along with the platoon, which is obviously inconsistent with conventional car-following models. Therefore, a few scholars are devoted to developing stochastic car-following models to capture the stochasticity of drivers. Laval et al. [45] proposed a parsimonious stochastic car-following model by adding white noise to the driver's expected acceleration in free flow. The results show that the model can produce traffic oscillations that are consistent with the observation results. Yuan et al. [46] developed a geometric Brownian-motion car-following model to explain the capacity drop. Based on the experimental data, Tian et al. [43] found that the growth of velocity difference oscillation follows the mean reversion process, and then they proposed a mode-switching stochastic car-following model. In addition, they also investigated the car-following behavior from the perspective of wave travel time and proposed a simple stochastic car-following model based on the Newell model [47]. Ngoduy et al. [38] modeled the driver's acceleration process as an extended Cox–Ingersoll–Ross stochastic process and derived the stability conditions of the stochastic car-following model for the first time. Furthermore, by introducing the stochasticity of drivers into the macroscopic traffic flow model, Ngoduy [48] proposed a class of stochastic high-order continuous traffic flow models and analyzed the stability of traffic flow under the influence of noise.

Although many researchers are devoted to capturing the driver's stochastic behavior by adding white noise to the acceleration function [38,45,46]; it does not reflect the relationship between stochasticity and some internal attributes of drivers (for example, some expectations or wishes of the driver during driving, which have a great impact on the driver's behavior and activities [49]); that is, the added white noise does not depend on some internal characteristics of the driver. However, Wagner [50,51] asserted that the random fluctuation of traffic flow is determined by the internal stochasticity of the driver itself. In addition, Makridis et al. [52] pointed out that the variation of the driver's desired velocity significantly impacts traffic flow stability. Therefore, it will be an interesting question of how the stochasticity of the driver's desired velocity influences the traffic flow stability.

To better describe the impact of the driver's internal stochasticity on car-following behavior, we use stochastic progress to describe the stochastic property of the driver's desired velocity and propose a stochastic FVDM (SFVDM). Furthermore, we propose a stable speed guidance model (S-SFVDM) based on the V2I environment. The driver's memory effect is considered to alleviate the traffic oscillation caused by driving stochasticity. We derive the stochastic stability conditions for the proposed models based on the stochastic differential equation. We prove that the S-SFVDM can rapidly enhance traffic stability by finding the close equilibrium position based on the stochastic stability diagram regarding the current state of instability.

The organization of the rest of this paper is as follows. Section 2 describes the formulation of the SFVMD and S-SFVDM. Section 3 derives the stochastic linear stability condition of two proposed models based on the Lyapunov stability analysis theory. In Section 4, numerical simulations are presented to verify the effectiveness of the developed models. Finally, the conclusions are summarized in Section 5.

2. Model formulation

The desired velocity of the driver, which has proved to have a significant impact on the stability of traffic flow, is affected by the inherent attributes of the driver, and it is closely related to the driver's age, personality, environment and other complex factors. Therefore, the driver's desired velocity is not a fixed value, but fluctuates randomly in a bounded range over time. It is one of the internal stochasticity of drivers. Hence, in this paper, the driver's desired velocity is considered as a stochastic process rather than assuming a constant value. Similarly, our model is based on the classical FVDM, which is given by

$$\frac{dv_n(t)}{dt} = \alpha\left[V_{op}\left(\triangle x_n(t)\right) - v_n(t)\right] + \lambda \triangle v_n(t) \tag{1}$$

where $v_n(t)$ is the n^{th} vehicle's velocity at time t. $\triangle v_n(t) = v_{n-1}(t) - v_n(t)$ and $\triangle x_n(t) = x_{n-1}(t) - x_n(t)$ are the velocity difference and distance between the n^{th} vehicle and the $(n\text{-}1)^{\text{th}}$ vehicle at time t, respectively. α, λ are the headway sensitivity coefficient and the velocity difference sensitivity coefficient of the driver, respectively. $V\left(\triangle x_n(t)\right)$ is the optimal velocity (OV) function, given by [38]:

$$V_{op}\left(\triangle x_n(t)\right) = \frac{v_0}{2}\left[tanh\left(\frac{\triangle x_n(t)}{h_0} - a\right) + tanh(a)\right] \tag{2}$$

where v_0 is the desired velocity of the driver, h_0 is the critical headway and a is a positive constant.

Yet, in reality, the desired velocity of a driver is not a constant, but fluctuates randomly in a bounded range over time with the dynamic variety of the driver's physiological and psychological properties. And, those properties are influenced by the external environment and many complex factors. To study the impact of the random variation of the desired velocity during stable traffic flow, we give the deterministic speed v_0 a stochastic term. Without losing generality, we propose the extended OV function as follows:

$$V_{op}^{S}\left(\triangle x_n(t)\right) = \frac{v_d^S}{2} \times \left[tanh\left(\frac{\triangle x_n(t)}{h_0} - a\right) + tanh(a)\right] \tag{3}$$

where v_d^S is the stochastic desired velocity, which is calculated as $v_0 + \xi\left(\triangle x_n(t), \gamma(t), v_n(t)\right)$. $\xi(\bullet)$ is the stochastic source, which depends not only on the state of the vehicle, but also on the stochastic progress $\gamma(t)$ at time t. When $\xi(\bullet) = 0$, $V_{op}^{S}\left(\triangle x_n(t)\right) = V_{op}\left(\triangle x_n(t)\right)$, which degenerates into Bando's OV function [3]. By taking the stochastic part $\xi(\bullet)$ into account in the FVDM, we develop the SFVDM, in which the Gaussian white noise is applied. By replacing $V_{op}\left(\triangle x_n(t)\right)$ with $V_{op}^{S}\left(\triangle x_n(t)\right)$ in Eq (1), we can reformat the SFVDM as

$$dv_n(t) = \alpha\left[V_{op}\left(\triangle x_n(t)\right) - v_n(t)\right]dt + \lambda \triangle v_n(t)dt + \alpha f\left(\triangle x_n(t)\right)\frac{1}{v_0}V_{op}\left(\triangle x_n(t)\right)dW(t) \tag{4}$$

where $W(t)$ is a Wiener process. $f\left(\triangle x_n(t)\right)$ is the diffusion coefficient function of the stochastic term, which indicates that the strength of the stochasticity depends on the value of the headway. According to the actual situation, we could know that when the headway is large, the driver will show a high degree of stochasticity, because the random fluctuation of headway does not affect driving safety. On

the contrary, when the headway is very small, drivers will drive carefully, so their stochasticity will remain at a low level. Hence, in this study, we consider the diffusion coefficient function $f\left(\triangle x_n\left(t\right)\right)$ of the stochastic term as follows:

$$f\left(\triangle x_n(t)\right) = \sigma\, tanh\left(\frac{\triangle x_n(t)}{h_0}\right) \tag{5}$$

Equation (5) endows the model with a good characteristic. Previous studies [39–44] suggested that there is no unique relationship between the space headway and the vehicle's velocity. In other words, drivers do not maintain a fixed space headway at a certain velocity, as they randomly change their preferred space headway [40–42]. In reality, we know that the smaller the space headway, the more cautious the driver will become. With the space headway increasing, drivers may have the opportunity to elevate the desired velocity. In Eq (5), if the spacing is far less than the safe distance (i.e., $\triangle x_n\left(t\right) \ll h_0$), $\tanh\left(\frac{\triangle x_n\left(t\right)}{h_0}\right)$ will become very small. Hence, $f\left(\triangle x_n\left(t\right)\right)$ will be minimally affected by the high value of the constant σ. In other words, the impact of the stochastic part on the desired velocity will be reduced largely in this situation.

Note that there is no consistent form of the diffusion coefficient function (i.e., Eq (5)) in previous studies [38–44,46,50], and it rarely affects the operation of vehicles [53]. On the one hand, the diffusion coefficient function developed in this paper guarantees a more reasonable acceleration with stronger non-negativity by integrating the driving state and traffic situation. On the other hand, it provides an opportunity to explore how the stochastic part in v_d^S influences traffic flow stability by deriving the string stability conditions.

Equation (5) can also describe the driver's stochastic desired velocity characteristics when the headway is relatively large. Even if the headway is far greater than the safe distance (i.e., $\frac{\triangle x_n\left(t\right)}{h_0} \gg 1$), the oscillation of the stochastic part is bounded. The function term $\sigma \tanh\left(\frac{\triangle x_n\left(t\right)}{h_0}\right)$ can enhance the non-negativity of the velocity and ensure that negative values of velocity are not easily generated as in other stochastic car-following models [45,46].

3. Linear stability analysis

Stability analysis is an important part of traffic flow research [6–12]. The stochastic nature of each driver will influence the stability of traffic flow. In order to understand the impact of random changes in the driver's desired speed on the stability of traffic flow, this section focuses on the investigation of the linear stability condition of the SFVDM.

3.1. Location stability analysis of SFVDM

Theoretically, each vehicle has the same velocity and space headway in the equilibrium state $\left(v_{equ}, x_{equ}\right)$, given by $v_1 = v_2 = v_3 = \cdots = v_{equ}$ and $x_1 = x_2 = x_3 = \cdots = x_{equ}$, where $v_{equ} = V\left(x_{equ}\right)$. To

derive the stability condition of the SFVDM, we put small disturbances ($\delta v_n(t) = v_n(t) - v_{equ}$ and $\delta x_n(t) = x_n(t) - x_{equ}$) on the velocity and space headway around the equilibrium state, respectively. The first-order Taylor expansion is used to linearize the stochastically perturbed evolution equation as follows:

$$\delta v_n(t) = \alpha\left[V_{op}'\delta x_n(t) - \delta v_n(t)\right]dt + \lambda\left(\delta v_{n-1}(t) - \delta v_n(t)\right)dt + \alpha\sigma\beta\delta x_n(t)dW(t) \tag{6}$$

where

$$\beta = \frac{1}{v_0}\left(tanh\left(\frac{x_{equ}}{h_0}\right)V_{op}' + \frac{V_{op}(x_{equ})}{h_0}\left(1 - tanh^2\left(\frac{x_{equ}}{h_0}\right)\right)\right) \tag{7}$$

In addition, the following equation could be obtained according to the definition and dynamics.

$$d\delta x_n(t) = [\delta v_{n-1}(t) - \delta v_n(t)]dt \tag{8}$$

A small disturbance may break the stable state of traffic flow under certain conditions and lead to local instability. The local stochastic stability analysis can help us understand the evolution of a small disturbance and how it leads to the local instability of the traffic flow. Based on the stochastic theory, the local stochastic stability condition is derived.

To simplify the analysis of the proposed model, Equations (6) and (8) can be formulated as a matrix equation, as follows:

$$d\mathrm{X}(t) = \mathrm{P}\mathrm{X}(t)dt + \mathrm{Q}\mathrm{X}(t)dW(t) \tag{9}$$

where

$$\mathrm{X}(t) = \begin{bmatrix}\delta x_n(t)\\ \delta v_n(t)\end{bmatrix} \tag{10}$$

$$\mathrm{P} = \begin{bmatrix}0 & -1\\ \alpha V_{op}' & -(\alpha+\lambda)\end{bmatrix} \tag{11}$$

$$\mathrm{Q} = \begin{bmatrix}0 & 0\\ \alpha\beta\sigma & 0\end{bmatrix} \tag{12}$$

Based on the Lyapunov stability theory [54,55], we have the definition below for studying the local stability of the SFVDM.

Definition 1. The trivial solution of Eq (9) is p^{th}-moment exponentially stable if there exist two constants c_1 , $c_2 \in (0,+\infty]$ and a Lyapunov function $V(\boldsymbol{X}(t))$ that satisfy the following two conditions:

$$c_1|\mathrm{X}(t)|^p \le V(\mathrm{X}(t)) \le c_2|\mathrm{X}(t)|^p \tag{13}$$

$$LV\big(\mathrm{X}(t)\big) < -\kappa V\big(\mathrm{X}(t)\big)\,, \kappa \geq 0 \tag{14}$$

Equations (13) and (14) are equivalent to the generally strict formulation, as follows:

$$\lim_{t\to\infty} t^{-1} E|\mathrm{X}(t)|^p < 0 \tag{15}$$

where

$$LV\big(\mathrm{X}(t)\big) = V_X\big(\mathrm{X}(t)\big)\mathrm{PX}(t) + \frac{1}{2} trace\left[\big(\mathrm{QX}(t)\big)^T V_{XX}\big(\mathrm{X}(t)\big)\mathrm{QX}(t)\right] \tag{16}$$

$$V_X\big(\mathrm{X}(t)\big) = \left(\frac{\partial V\big(\mathrm{X}(t)\big)}{\partial \delta v_n(t)}, \frac{\partial V\big(\mathrm{X}(t)\big)}{\partial \delta x_n(t)}\right)^T \tag{17}$$

$$V_{XX}\big(\mathrm{X}(t)\big) = \begin{pmatrix} \dfrac{\partial^2 V\big(\mathrm{X}(t)\big)}{\partial \delta v_n(t)\delta v_n(t)} & \dfrac{\partial^2 V\big(\mathrm{X}(t)\big)}{\partial \delta v_n(t)\delta x_n(t)} \\ \dfrac{\partial^2 V\big(\mathrm{X}(t)\big)}{\partial \delta x_n(t)\delta v_n(t)} & \dfrac{\partial^2 V\big(\mathrm{X}(t)\big)}{\partial \delta x_n(t)\delta x_n(t)} \end{pmatrix} \tag{18}$$

Based on Definition 1, we have the following theorem:

Theorem 1. The SFVD model is 2nd-moment exponentially stable if

$$\sigma^2 \leq \frac{2(\alpha+\lambda)V'}{\alpha\beta^2} \tag{19}$$

Proof. Based on the Lyapunov stability theory, the Lyapunov function is set as

$$V\big(\mathrm{X}(t)\big) = \big(\mathrm{X}^T(t)\mathrm{FX}(t)\big)^{\frac{p}{2}} \tag{20}$$

According to the definition of $LV\big(\boldsymbol{X}(t)\big)$, if the matrix F is positive-definite, $LV\big(\boldsymbol{X}(t)\big)$ can be reformatted as

$$LV\big(X(t)\big) = p\big(X(t)^T FX(t)\big)^{\frac{p}{2}-1}\big(X(t)^T FPX(t)\big) + \frac{p(p-2)}{2}\big(X(t)^T FX(t)\big)^{\frac{p}{2}-2}\left|\big(QX(t)\big)^T GQX(t)\right|^2 + \frac{1}{2} trace\Big(\big(QX(t)\big)^T FQX(t)\Big) \tag{21}$$

Then, we set $p = 2$, $\kappa = 0$ and $\boldsymbol{F}$ as follows:

$$\mathrm{F} = \begin{bmatrix} \alpha V' + \dfrac{1}{2}(\alpha+\lambda)^2 & \dfrac{-(\alpha+\lambda)}{2} \\ \dfrac{-(\alpha+\lambda)}{2} & 1 \end{bmatrix} \tag{22}$$

The Lyapunov function is

$$V(\mathrm{X}(t)) = \left[\alpha V' + \frac{1}{2}(\alpha+\lambda)^2\right]\delta x_n{}^2(t) - (\alpha+\lambda)\delta x_n(t)\delta v_n(t) + \delta v_n{}^2(t) \quad (23)$$

Furthermore,

$$LV(\mathrm{X}(t)) = [\alpha^2\beta^2\sigma^2 - (\alpha+\lambda)\alpha V']\delta^2 x_n(t) - \frac{(\alpha+\lambda)}{2}\delta^2 v_n(t) \quad (24)$$

If $LV(\boldsymbol{X}(t)) \le 0$, Equation (14) holds. Equation (13) is also satisfied by setting the values of c_1 and c_2 as follows:

$$c_1 = -\frac{1}{2}\sqrt{\left(\alpha V' + \frac{1}{2}(\alpha+\lambda)^2 + 1\right)^2 - 4\left[\alpha V' + \frac{1}{4}(\alpha+\lambda)^2\right]} + \frac{1}{2}\left(\alpha V' + \frac{1}{2}(\alpha+\lambda)^2 + 1\right) \quad (25)$$

$$c_2 = \frac{1}{2}\sqrt{\left(\alpha V' + \frac{1}{2}(\alpha+\lambda)^2 + 1\right)^2 - 4\left[\alpha V' + \frac{1}{4}(\alpha+\lambda)^2\right]} + \frac{1}{2}\left(\alpha V' + \frac{1}{2}(\alpha+\lambda)^2 + 1\right) \quad (26)$$

3.2. String stability analysis of SFVDM

The string stability analysis of the SFVDM explains how a small disturbance propagates from the first leading vehicle to the last vehicle in a platoon. If the string stability condition is satisfied, any small disturbance will be weakened from the leading vehicle to the next following vehicle and the strength of random fluctuations will be decreased continuously in traffic flow.

We expand $\delta v_n(t) = \zeta_1 e^{in\omega+zt}$ and $\delta x_n(t) = \zeta_2 e^{in\omega+zt}$ in Eq (6), where ζ_1 and ζ_2 are two constants. Then, the SFVDM can also be treated as the linear stochastic ordinary difference equation:

$$d\mathrm{X}(t) = \widetilde{\mathrm{P}}\mathrm{X}(t)dt + \mathrm{Q}\mathrm{X}(t)dW(t) \quad (27)$$

where

$$\widetilde{\mathrm{P}} = \begin{bmatrix} 0 & e^{-i\omega} - 1 \\ \alpha V' & -\alpha - \lambda + \lambda e^{-i\omega} \end{bmatrix} \quad (28)$$

To study the string stability of the proposed stochastic car-following model, Theorem 2 is given to study the moment exponential stability of the traffic flow.

Theorem 2. The stochastic car-following model is 2nd-moment exponentially stable if

$$\sigma^2 < \frac{2\left[\alpha+\lambda-\sqrt{\lambda^2+2\alpha V_{op}{}'}\right]}{\alpha^2\beta^2} \quad (29)$$

Proof. According to Definition 1, by incorporating Eq (27) into Eq (21) and setting $p = 2$, we can obtain the characteristic equation of the system as follows:

$$z^2 - z[-\alpha + \lambda(e^{-i\omega} - 1) + 0.5\alpha^2\beta^2\sigma^2] - \alpha V'(e^{-i\omega} - 1) = 0 \quad (30)$$

Expanding $z = i\omega z_1 + \omega^2 z_2 + \cdots$ into Eq (30) and ignoring the high-order terms, the expressions of z_1 and z_2 can be obtained as follows by setting the first-order and second-order terms to be zero:

$$z_1 = \frac{-\alpha V_{op}'}{\alpha - \frac{1}{2}\alpha^2\beta^2\sigma^2} \tag{31}$$

$$z_2 = \frac{z_1^2 + \lambda z_1 - \frac{1}{2}\alpha V'}{\alpha - \frac{1}{2}\alpha^2\beta^2\sigma^2} \tag{32}$$

The condition of stochastic stability will be held if $z_1 < 0$ and $z_2 < 0$. Hence, we can obtain the stability conditions by treating σ as the variable:

$$\sigma^2 < \frac{2\left[\alpha + \lambda - \sqrt{\lambda^2 + 2\alpha V_{op}'}\right]}{\alpha^2\beta^2} \tag{33}$$

It is worth mentioning that, if $\sigma = 0$, the SFVDM will degenerate to the FVDM. In the meantime, the stochastic stability condition will become $V_{op}' < \frac{\alpha}{2} + \lambda$, which is the stability condition of the FVDM.

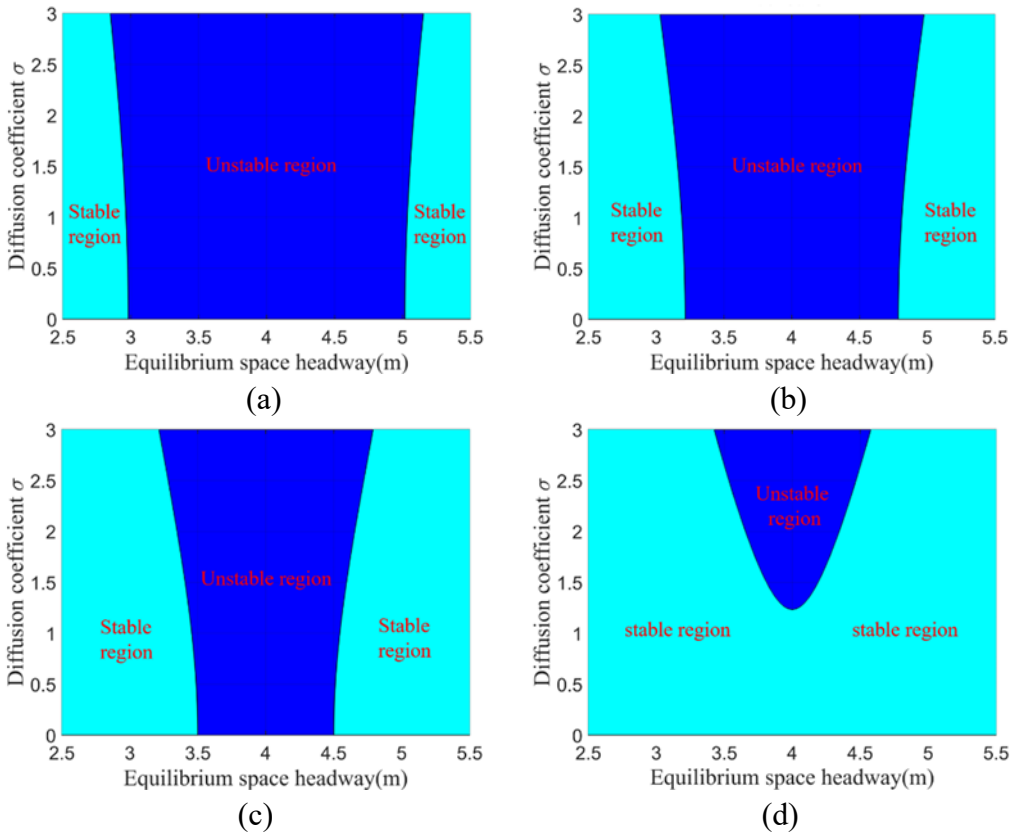

Figure 1. Stability region of SFVDM with different values of λ, where (a) $\lambda = 0.24$, (b) $\lambda = 0.28$, (c) $\lambda = 0.32$ and (d) $\lambda = 0.36$.

Figure 1 shows the stability diagrams for the SFVDM with different values of the velocity difference sensitivity coefficient λ, where the values of λ in Figure 1(a)–(d) are 0.24, 0.28, 0.32 and 0.36, respectively. Other parameters of the SFVDM were set as $\alpha = 0.3s^{-1}$, $h = 2m$ and $V_{\exp} = 2m/s$. In Figure 1, it is shown that the coverage of the unstable region decreases as the value of λ increases.

Figure 2 shows the stability diagrams for the FVDM. Note that Figure 1d and Figure 2 have the same value of λ (i.e., $\lambda = 0.36$). In Figure 2, the traffic flow is always in a stable state when $\alpha > 0.28$. In Figure 1(d), the traffic flow is in the stable regime when $\sigma < 1.2$, but it is always in the unstable region when $\sigma > 1.2$. It clearly indicates that the stochasticity has a significant potential negative impact on the stability of traffic flow. When the random noise strength exceeds a threshold value, the traffic flow will become unstable. In addition, when λ is a relatively small value (e.g., $\lambda < 0.32$), a small value of σ will result in instability of the traffic flow with headways between 3.5 and 4 m. It indicates that the driver's stochasticity will decrease the stability of the traffic flow.

According to the above analysis, we can observe that the stochastic desired velocity of the driver is a critical factor that induces the instability of the traffic flow. This result is consistent with the findings in the previous study [52]. Therefore, it is necessary to design a control strategy to reduce the negative impacts of stochastic driving properties on the traffic flow. V2I communication technology can realize the information interaction between vehicles and roadside facilities within an effective range, which provides a prerequisite for speed guidance. In the next section, a stable speed guidance strategy is proposed considering the driver's memory effect, as based on the V2I environment, to address the above issue.

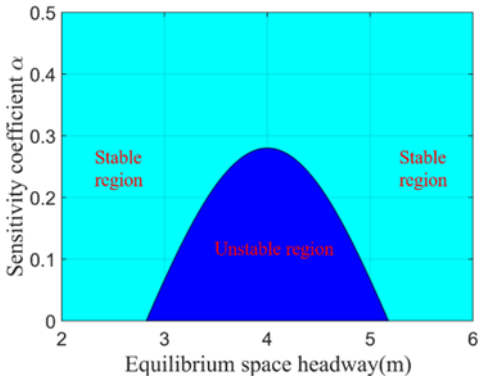

Figure 2. Stability region of FVDM.

4. Stable speed guidance model (S-SFVDM) based on V2I environment

The development of V2I communication technology allows us to alleviate the traffic oscillation caused by the driver's stochastic nature. In this section, we propose an S-SFVDM to reduce the effect of the driver's randomly desired velocity based on the V2I environment. We consider the potential influence of the driver's short-term memory on the speed guidance. We assume that all vehicles can communicate with the intelligent roadside system that can capture all vehicles' speeds, locations and other useful information at each time step (communication delay will not be considered in this study).

Based on the stability diagram, it is easy to find the point $e(\overline{x}_t, \sigma)$ by fixing σ at any time step, where $\overline{x}_t$ denotes the mean value of the space headway of all vehicles at time t. The essential idea is

that it is easy to find the equilibrium point e' nearest to the current point e in the unstable region as the expected state for when the platoon will arrive after the speed guidance. And, this process is real-time and dynamic.

The stable speed guidance strategy is described using the following equations:

$$dv_n(t) = \alpha\left[V_{op}\left(\triangle x_n(t)\right) - v_n(t)\right]dt + \lambda \triangle v_n(t)dt + \alpha\sigma \tanh\left(\frac{\triangle x_n(t)}{h_0}\right)\frac{1}{v_0}V_{op}\left(\triangle x_n(t)\right)dW(t)$$
$$+\phi(\eta[g(\bar{x}_t) - \tau\sum_{k=0}^{Ts} f_\Gamma(k\tau)v_n(t-k\tau)] + (1-\eta)[g(\bar{x}_t) - \tau\sum_{k=0}^{Ts} f_\Gamma(k\tau)v_{n-1}(t-k\tau)]) \quad (34)$$

$$g(\bar{x}_t) = V_{op}^S(\bar{x}_t) \quad (35)$$

where ϕ denotes the mean value of the compliance of drivers to the speed guidance. $\eta \in [0.5,1]$ indicates that the weight of the target vehicle in the speed guidance strategy is greater than the preceding vehicle. τ is the length of each memory interval. ϕ , τ and η are all constants. $g\left(\overline{x}_t\right)$ denotes the of guidance speed computed by the intelligent roadside system.

The driver's memory effect is assumed to be homogeneous in many studies. It can potentially incur unrealistic phenomena. For example, when the length of the time period of the driver's historical memory is a relatively large value, the car-following system will be stable regardless of the value of the sensitivity. One reason leading to this problem is that the memory effect of drivers should decay to zero when the time increases to a large value. In order to better describe the actual situation, the memory effect of drivers is considered as a gamma distribution [21,22] in this paper.

$$f_\Gamma(\omega) = \frac{u^m \omega^{m-1} e^{-u\omega}}{\Gamma(u)} \quad (36)$$

$$\Gamma(u) = \int_0^{+\infty} x^{u-1}e^{-x}dx \quad (37)$$

When a vehicle is in the steady state, under critical conditions, Equation (33) can be formulated as

$$\sigma(\Delta x) = \frac{2}{\alpha\beta}\sqrt{\alpha + \lambda - \sqrt{\lambda^2 + 2\alpha V_{op}{}'}} \quad (38)$$

The stability diagrams show that the function $\sigma\left(\Delta x\right)$ is monotonic both in the left part and the right part. It is decreasing in the left parts and increasing in the right parts. Figure 3 gives the sketch map of the stable speed guidance strategy based on the stable diagram. The intention for this study was to identify a reasonable and effective guidance velocity which can facilitate the process of stabilizing traffic flow. More specifically, we first calculate the average headway $\Delta\overline{x}$ of traffic flow and find the

point $e_t'(\Delta\hat{x},\sigma_t)$, which is the closest position of the stable regime to $e_t(\Delta\bar{x},\sigma_t)$ with a fixed σ_t. The expression of neutral stable curves C_1 and C_2 are already obtained so that we can derive the point $e_t'(\Delta\hat{x},\sigma_t)$ by calculating d_t^1 and d_t^2 ($d_t^1 \le d_t^2$). To calculate d_t^i accurately, we use the simple least squares method to compute the intersection $e_t'(\Delta\hat{x},\sigma_t)$. The relationship between iteration error and iteration times is as follows:

$$\frac{b_{up}-b_{low}}{2^{j_{iter}+1}} < \varepsilon \tag{39}$$

where j_{iter} is the number of iterations and ε is the iterative error.

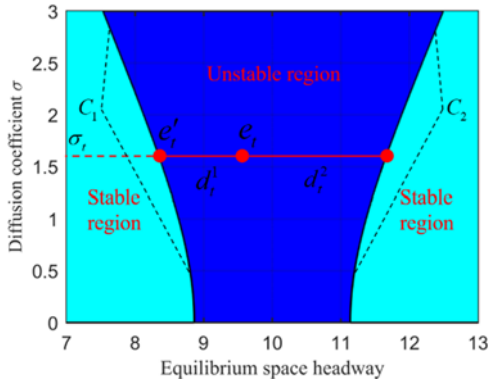

Figure 3. Sketch map of stable speed guidance strategy based on the stable diagram in equilibrium space headway-diffusion coefficient space under the conditions of the V2I environment.

If there is a small deviation from the equilibrium state, the function $g(\bar{x}_t)$ could be treated as a constant. The stability analysis can be explored in this situation, as the results display how the speed guidance under the conditions of the V2I environment influence the stability of traffic considering driver memory. Therefore, in the next step, the stability analysis of the expanded stochastic model will be deduced. For simplicity, we give the stability condition directly by omitting the details here, and the detailed derivation process is given in Appendix A.

The S-SFVDM is considered to be 2nd-moment exponentially stable if

$$\sigma^2 < \frac{4\left(\alpha+\lambda+\phi\eta\tau\sum_{k=0}^{Ts} f_\Gamma(k\tau)-\sqrt{\left[\lambda-\phi(1-\eta)\tau\sum_{k=0}^{Ts} f_\Gamma(k\tau)\right]^2+2\left(1-\phi\tau^2\sum_{k=0}^{Ts} k f_\Gamma(k\tau)\right)\alpha V_{op}'}\right)}{\alpha^2\beta^2} \tag{40}$$

Later, we will find that, compared with the SFVDM, the S-SFVDM has a larger stability region due to considering the speed guidance strategy.

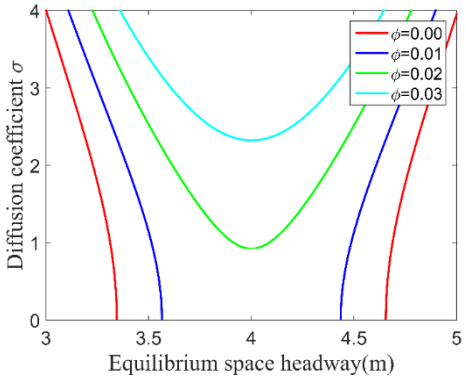

Figure 4. Stable diagram in equilibrium space headway-diffusion coefficient space for different values of ϕ.

Figure 4 shows the neutral stability curves for different values of ϕ. The region enclosed by the curve and coordinate axis is the stable region of the traffic flow, and all other regions are the unstable region of the traffic flow. Figure 4 indicates that, with the increase of ϕ, the stability of the stochastic car-following model becomes stronger. It further indicates that providing effective speed guidance information to the driver, given that the driver's memory is considered, is beneficial to the improvement of the stability of traffic flow based on V2I technology. This result is consistent with many findings of relevant studies [21–26].

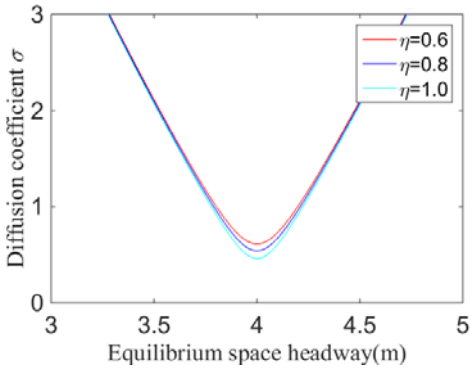

Figure 5. Stable diagram in equilibrium space headway-diffusion coefficient space for different values of $\eta(0.6,\ 0.8,\ 1.0)$.

Figure 5 describes the neutral stability curves for different values of η. The region enclosed by the curve and coordinate axis is the stable region of the traffic flow, and all other regions are the unstable region of the traffic flow. It can be seen in Figure 5 that the stability of the traffic flow increases with the decrease of η, which indicates that considering the dynamics of the preceding vehicle for the target vehicle in the speed guidance strategy is conducive to improving the stability of the traffic flow. In addition, we can also find that a change in η has a limited impact on the stability of traffic flow.

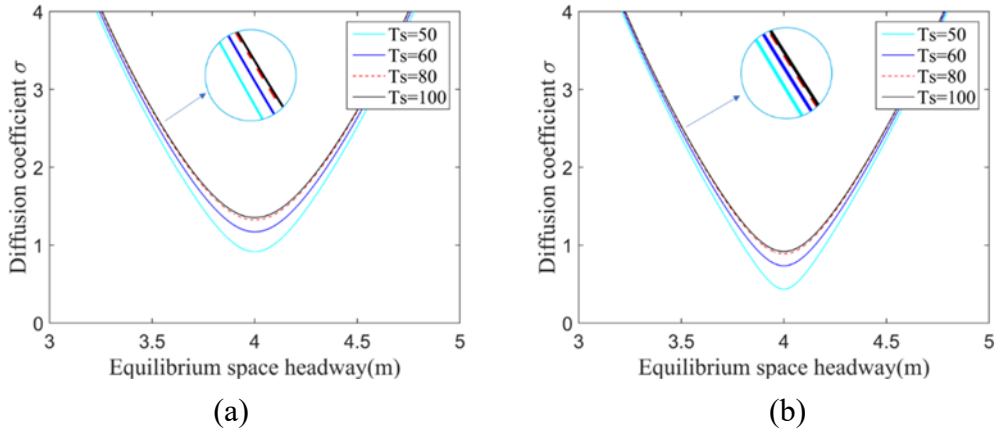

Figure 6. Stable diagram in equilibrium space headway-diffusion coefficient space for different values of *Ts* and different parameter settings, where (a) $\lambda = 0.28, \phi = 0.03$ and (b) $\lambda = 0.3, \phi = 0.02$.

Figure 6 displays the stable diagram in equilibrium space headway-diffusion coefficient space for different values of *Ts*, where (a) $\lambda = 0.28, \phi = 0.03$ and (b) $\lambda = 0.3, \phi = 0.02$. The region enclosed by the curve and coordinate axis is the stable region of the traffic flow, and all other regions are the unstable region of the traffic flow. It indicates that the area of the stability region increases with increasing driver memory time. In addition, Figure 6 shows that the increase in the stability regime gradually converges with the elongation of the driver's memory time. Meanwhile, taking the driver's memory into account is more reasonable [21,22].

5. Numerical simulations

In order to validate the accuracy of the theoretical analysis and the superiority of the proposed models, numerical simulations were carried out under a periodic boundary condition. We assumed that all vehicles run on a ring road and have the same initial headway, as well as the same velocity. For simplicity, we applied the explicit Euler–Maruyama scheme to discretize the stochastic differential equation. The numerical approximation of the SFVDM is

$$v_n(k+1) - v_n(k) = \alpha\left[V_{op}(\Delta x_n(k)) - v_n(k)\right]\Delta t + \alpha\sigma tanh\left(\frac{\Delta x_n(k)}{h_0}\right)\frac{1}{v_0}V_{op}(\Delta x_n(k))\sqrt{\Delta t}\Delta W(k+1) + \lambda \triangle v_n(k)\Delta t \quad (41)$$

Based on the proposed SFVDM, we first carried out a series of simulations of platoon with different numbers of vehicles under the open boundary condition (i.e., on a straight road of infinite length). The model parameters were as follows:

$$\alpha = 0.3\,, \lambda = 0.3\,, h_0 = 15m\,, v_0 = 20m/s, \sigma = 1 \quad (42)$$

The standard deviations of the speed profiles and fitting curves of different simulations are shown in Figure 7. The number of vehicles in each sub-figure are (a) 50 vehicles, (b) 100 vehicles, (c) 150 vehicles and (d) 200 vehicles. In Figure 7, the black points represent the standard deviation of each vehicle's velocity in the platoon, and the blue lines are quadratic polynomial fitting curves in different

simulations. Figure 7 shows an interesting property of the SFVDM, where the profiles of the standard deviations of speed are concave curves, which are consistent with empirical data [38–43,52].

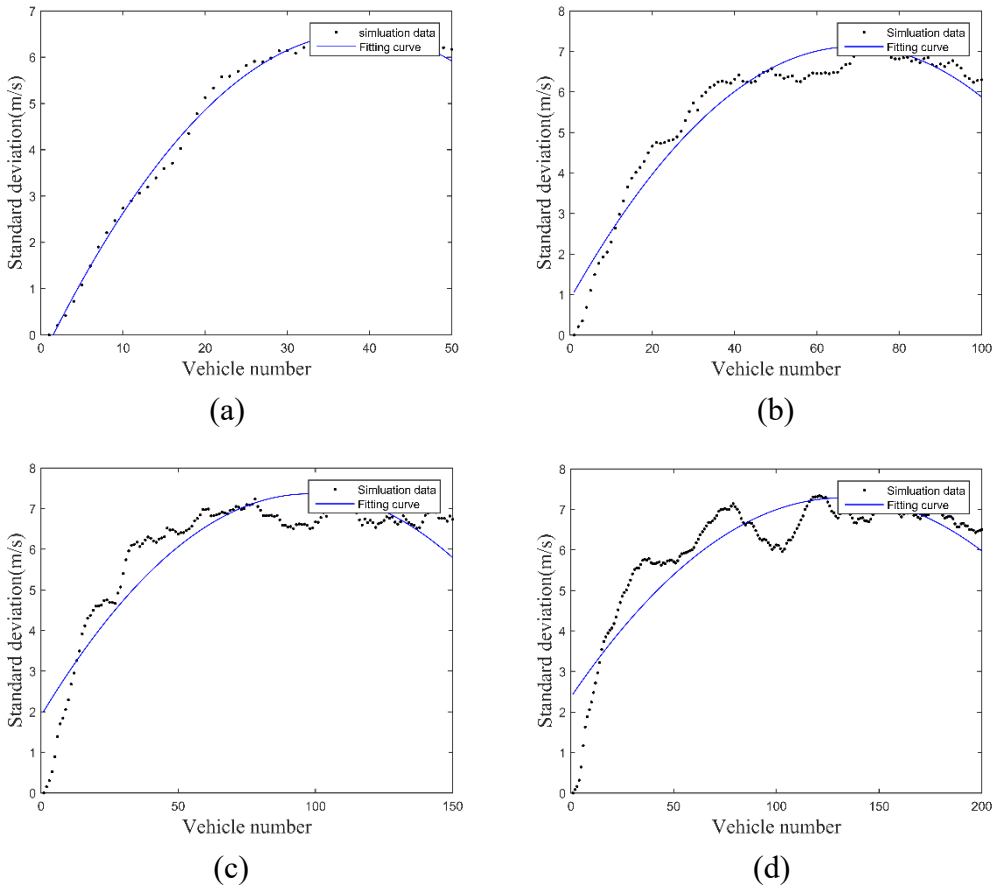

Figure 7. Standard deviations of speed profiles and fitting curves for different simulated numbers of vehicles, where (a) 50 vehicles, (b) 100 vehicles, (c) 150 vehicles and (d) 200 vehicles.

To further verify the SFVDM and S-SFVDM, we conducted a series of simulations under the periodic boundary condition (i.e., on a ring road). The initial parameters are given as follows: the vehicle number $N = 100$, the road length $L = 400m$ and the time step of the simulation was 0.1 s. Other parameters were set as follows:

$$\alpha = 0.3\,, \lambda = 0.3\,, \eta = 0.7\,, h_0 = 2m\,, v_0 = 2m/s\,, a = 2\,, t = 3000s \tag{43}$$

$$x_1(0) = L - \frac{L}{N} \tag{44}$$

$$x_n(0) = (N - n)\frac{L}{N}(n = 2,3,4,\cdots,N) \tag{45}$$

$$v_1(t) = v_2(t) = \cdots = v_n(t) = v_e = V_{op}\left(\frac{L}{N}\right) \tag{46}$$

$$v_1(20/\tau) = 0.9v_e \tag{47}$$

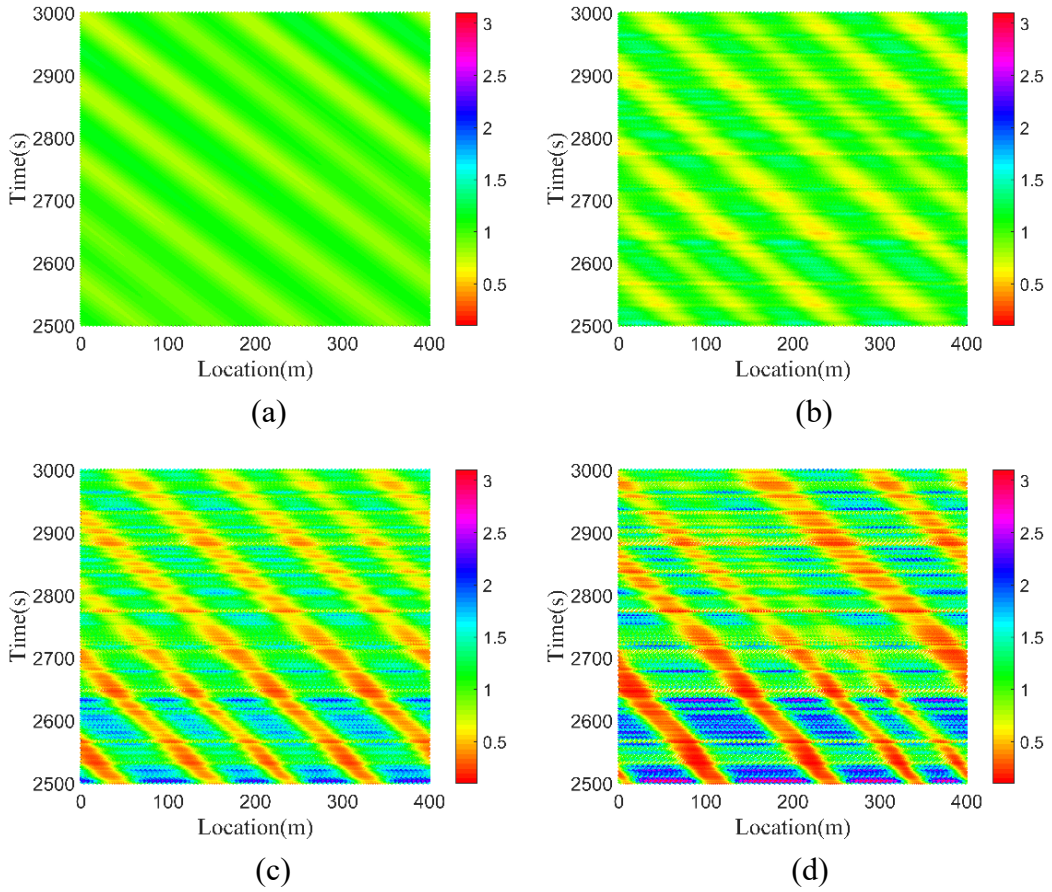

Figure 8. Time-space evolutions of all vehicles for different values of σ, where (a) $\sigma = 0$, (b) $\sigma = 0.5$, (c) $\sigma = 1$ and (d) $\sigma = 1.5$.

Figure 8 shows the time-space evolutions of the platoon for different values of the diffusion coefficient $\sigma = 0,\ 0.5,\ 1,\ 1.5$, with the color representing vehicle velocity. From Figure 8, it can be found that, with the increase of σ, the oscillation of velocity becomes larger. In addition, higher stochasticity leads to more vehicles staying at a low-velocity state for a longer period. It indicates that the increasing stochasticity of drivers leads to stronger instability of traffic flow and more frequent stop-and-go phenomena. Furthermore, with the increase in the intensity of the randomness of the driver's desired velocity, the density wave of traffic flow becomes more uneven.

Figure 9 shows the time-space evolutions of the headway profile for different values of σ. In Figure 9, λ is equal to 3.0, and the headway is equal to 3.2 m. According to Theorem 2, the boundary of stability is $2 < \sigma = 2.276 < 2.5$. In Figure 9(a), large uneven oscillations occur in the headway and the traffic flow is extremely unstable. On the contrary, the headway is steady without fluctuation in Figure 9(b), and the traffic flow is stochastically stable. The simulation results are consistent with the stability boundary conditions.

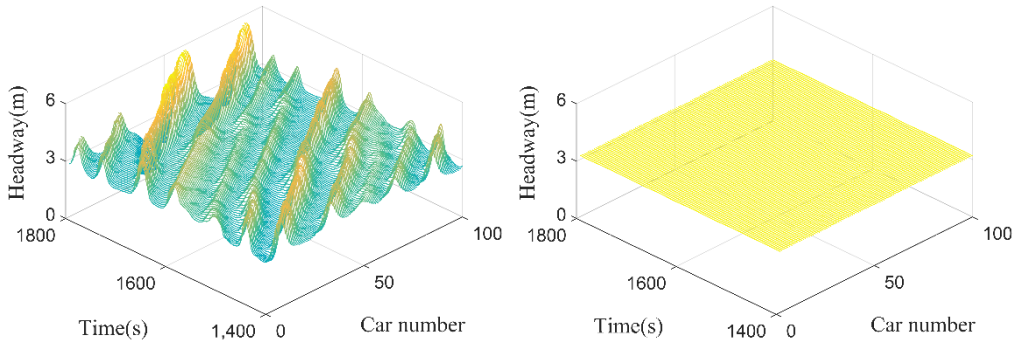

(a) (b)

Figure 9. Time-space evolutions of the headway profile after a sufficient time $t = 1400s$, where (a) $\sigma = 2.5$ and (b) $\sigma = 2.0$.

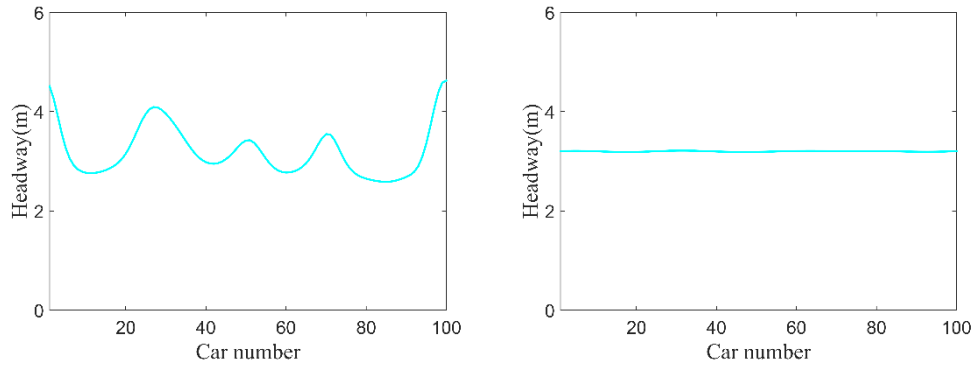

(a) (b)

Figure 10. Snapshots of headway configuration of all vehicles at time $t = 1650s$, where (a) $\sigma = 2.5$ and (b) $\sigma = 2.0$.

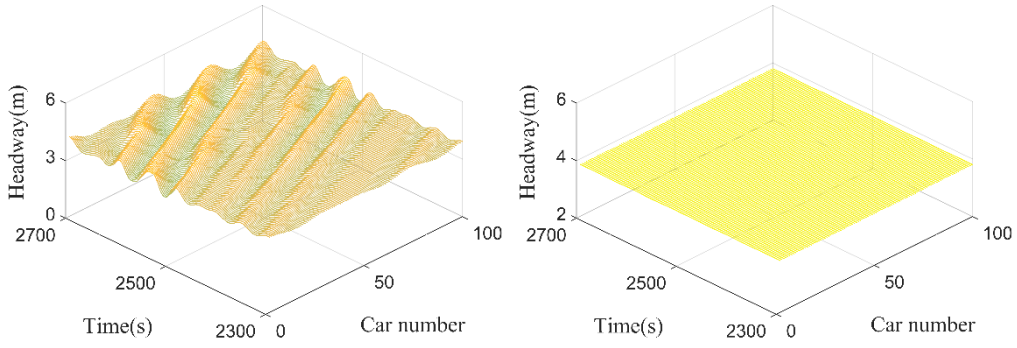

(a) (b)

Figure 11. Time-space evolutions of the headway profile after a sufficient time $t = 2300s$, where (a) $\sigma = 2.0$ and (b) $\sigma = 1.0$.

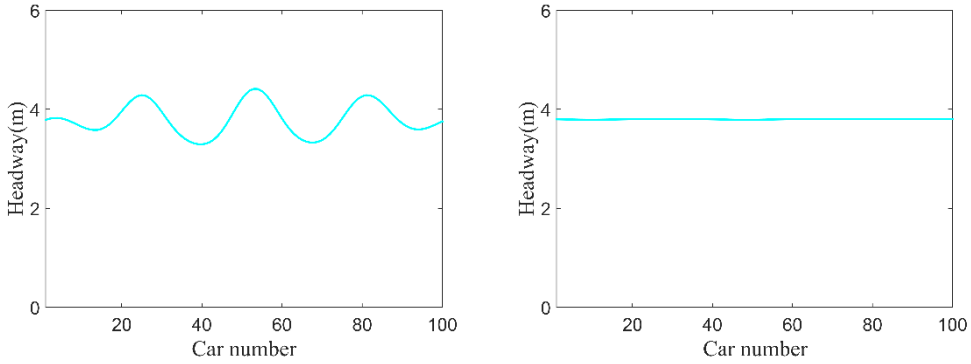

(a) (b)

Figure 12. Snapshots of headway configuration of all vehicles at time $t = 2650s$, where (a) $\sigma = 2.0$ and (b) $\sigma = 1.0$.

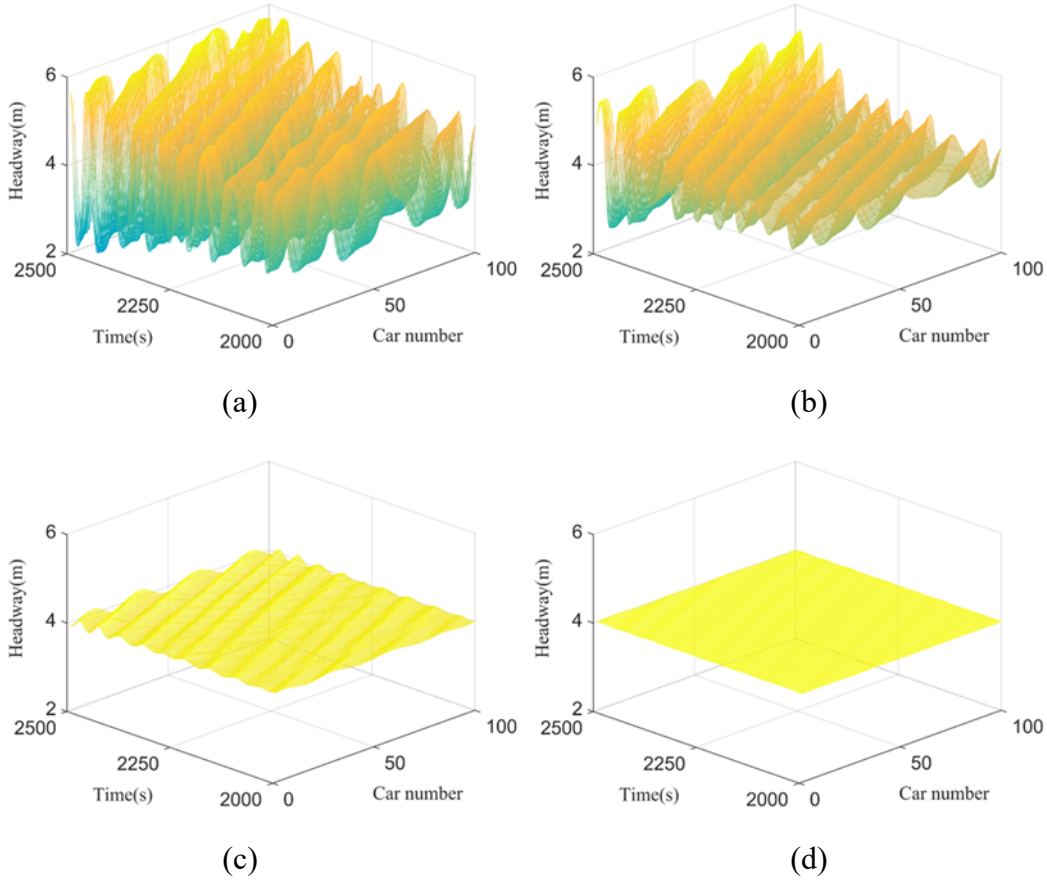

(a) (b)

(c) (d)

Figure 13. Time-space evolutions of the headway profiles for different values of ϕ, where (a) $\phi = 0.00$, (b) $\phi = 0.01$, (c) $\phi = 0.02$ and (d) $\phi = 0.03$.

Figure 10 shows the snapshots of the headway configuration of all vehicles at time $t = 1650s$ for different values of σ. It shows that the headway oscillations in Figure 10(a) are severe. However, the headway profile in Figure 10(b) approximates a straight line. Similarly, we also verify the correctness of the stability condition under another condition.

As shown in Figures 11 and 12, the time-space evolutions of the headway profile and snapshots of the headway configuration of all vehicles at time $t = 2650s$ were both used to further test the correctness of the stability conditions. According to Eq (33), when $\lambda = 0.36$ and the headway is equal to 3.8 m, the stable boundary condition is $1 < \sigma = 1.528 < 2$. It indicates that the traffic flow is unstable when $\sigma = 2$, and that the traffic flow is in the string stability regime when $\sigma = 1$, which are in line with the numerical simulation results revealed in Figures 11 and 12. Moreover, these results suggest that the driver's stochastically desired velocity will decrease the stability of traffic flow. However, with the increase of the stochasticity strength, the stable regime will further reduce and the oscillation of traffic flow tends to become more serious. Therefore, the random variation of the driver's desired velocity is one of the important reasons for traffic oscillation.

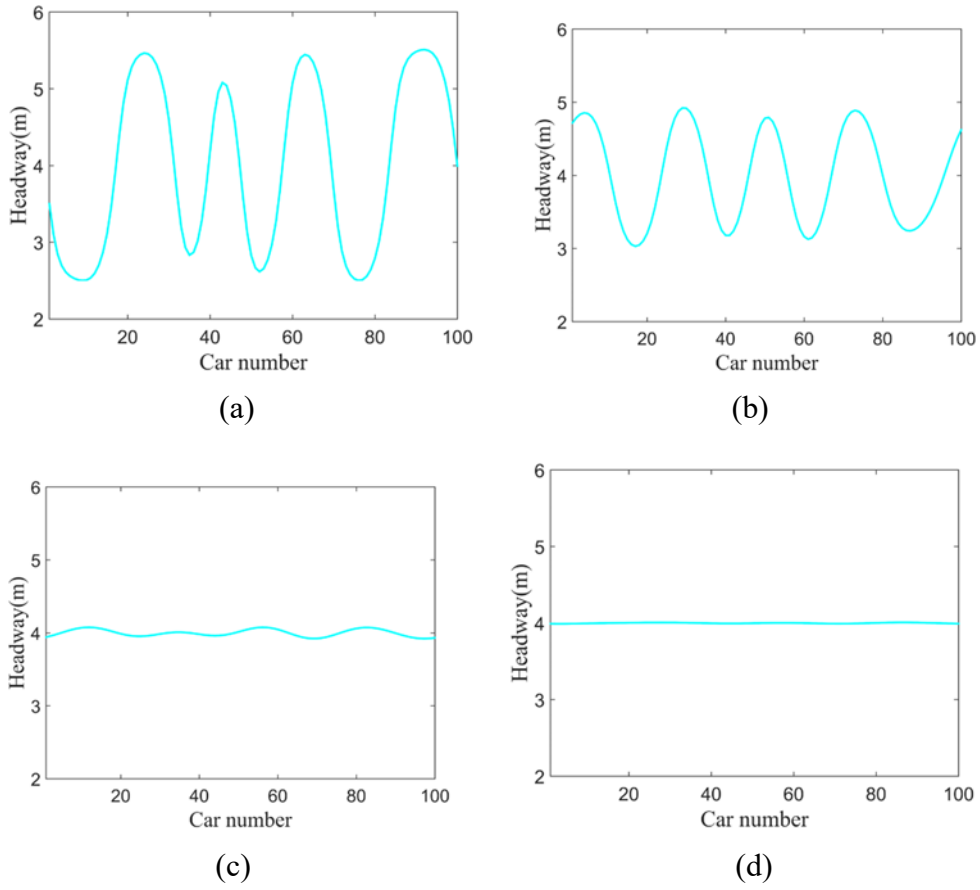

Figure 14. Snapshots of headway configuration of all vehicles at time $t = 2350s$ for different values of ϕ, where (a) $\phi = 0.00$, (b) $\phi = 0.01$, (c) $\phi = 0.02$ and (d) $\phi = 0.03$.

Figure 13 presents the time-space evolutions of the headway profiles for $\phi = 0.00, 0.01, 0.02, 0.03$. Drivers do not receive the speed guidance information when $\phi = 0$. The amplitude of the headway profile is considerable and traffic flow is volatile. With the increase of ϕ, the amplitude of the headway profile decays obviously. It indicates that the fluctuation of traffic flow decreases with the increase of ϕ. When $\phi = 0.03$, the traffic flow is stochastically stable. Figure 14 shows snapshots of the headway configuration of all vehicles at time $t = 2350s$ for different values of ϕ, which shows the same results as Figure 13.

Meanwhile, we can conclude from the above diagrams that giving equilibrium speed guidance to

the driver can effectively reduce the instability of traffic flow caused by the random change of the driver's desired velocity. Compared with the SFVDM, the proposed S-SFVDM based on the V2I environment has a larger stable region. Moreover, the negative impact of the stochasticity of the driver's desired velocity can be abated effectively by stable speed guidance. The numerical simulation results are consistent with the theoretical analysis results.

6. Conclusions

In this study, a stochastic car-following model, i.e., an SFVDM, was developed to explore the impact of human expectation uncertainty of velocity on traffic stability. The desired velocity of the driver was considered as a stochastic process. The magnitude of the stochasticity is related to the traffic condition, which determines the non-negativity of the vehicle's velocity in most cases. Stochastic stability analysis was simulated to observe the conditions of local stability and string stability of traffic flow. The results demonstrate that the driver's stochastic desired velocity will decrease the coverage of the stable regime. To reduce the negative effects of the internal stochasticity of the driver, we developed a stable speed guidance strategy, i.e., the S-SFVDM, based on the V2I environment. Furthermore, the driver's memory effect is considered as a gamma distribution to fit the actual situation better. Numerical simulations were carried out to validate the proposed models. The results indicate that the stability of traffic flow can be enhanced effectively by applying the proposed stable speed guidance strategy. Specifically, sending a stable guidance velocity to each driver can weaken the negative influence brought about by the driver's stochastic nature.

However, the main work of this paper focuses on the model formulation and the derivation of the stochastic stability analysis of the proposed model. The model parameters were not calibrated based on field or experimental data. In future research, we will conduct car-following experiments to validate the numerical results and calibrate the model parameters. In addition, modeling and analysis of heterogeneous traffic flow that mixes regular and connected vehicles with the stochastic nature of humans are also further research directions.

Acknowledgments

This work was supported by the National Natural Science Foundation of China (72201010) and the China Postdoctoral Science Foundation (2021M700304).

Conflict of interest

The authors declare that there is no conflict of interest.

References

1. G. F. Newell, Nonlinear effects in the dynamics of car following, *Oper. Res*., **9** (1961), 209–229.
2. M. Bando, K. Hasebe, A. Nakayama, Y. Shibata, Y. Sugiyama, Dynamical model of traffic congestion and numerical simulation, *Phys. Rev. E*, **51** (1995), 1035. https://doi.org/10.1103/PhysRevE.51.1035

3. D. Helbing, B. Tilch, Generalized force model of traffic dynamics, *Phys. Rev. E*, **58** (1998), 133. https://doi.org/10.1103/PhysRevE.58.133
4. R. Jiang, Q. Wu, Z. Zhu, Full velocity difference model for a car-following theory, *Phys. Rev. E*, **64** (2001), 017101. https://doi.org/10.1103/PhysRevE.64.017101
5. S. Yu, Z. Shi, Dynamics of connected cruise control systems considering velocity changes with memory feedback, *Measurement*, **64** (2015), 34–48. https://doi.org/10.1016/j.measurement.2014.12.036
6. J. Chen, R. Liu, D. Ngoduy, Z. K. Shi, A new multi-anticipative car-following model with consideration of the desired following distance, *Nonlinear Dyn.*, **85** (2016), 2705–2717. https://doi.org/10.1007/s11071-016-2856-4
7. C. Jiang, R. Cheng, H. Ge, An improved lattice hydrodynamic model considering the "backward looking" effect and the traffic interruption probability, *Nonlinear Dyn.*, **91** (2018), 777–784. https://doi.org/10.1007/s11071-017-3908-0
8. T. Tang, H. Huang, S. Zhao, G. Xu, An extended OV model with consideration of driver's memory, *Int. J. Mod. Phys. B.*, 23 (2009), 743–752. https://doi.org/10.1142/S0217979209051966
9. D. Liu, Z. Shi, W. H. Ai, Enhanced stability of car-following model upon incorporation of short-term driving memory, *Commun. Nonlinear Sci. Numer. Simul.*, **47** (2017), 139–150. https://doi.org/10.1016/j.cnsns.2016.11.007
10. S. Yu, J. Tang, Q. Xin, Relative velocity difference model for the car-following theory, *Nonlinear Dyn.*, **91** (2018), 1415–1428. https://doi.org/10.1007/s11071-017-3953-8
11. S. Yu, M. Huang, J. Ren, Z. Shi, An improved car-following model considering velocity fluctuation of the immediately ahead car, *Physica A*, **449** (2016), 1–17. https://doi.org/10.1016/j.physa.2015.12.040
12. S. Yu, Z. Shi, An improved car-following model considering headway changes with memory, *Physica A*, **421** (2015), 1–14. https://doi.org/10.1016/j.physa.2014.11.008
13. C. Chen, R. Cheng, H. Ge, An extended car-following model considering driver's sensory memory and the backward looking effect, *Physica A*, **525** (2019), 278–289. https://doi.org/10.1016/j.physa.2019.03.099
14. Y. Wang, H. Song, R. Cheng, TDGL and mKdV equations for an extended car-following model with the consideration of driver's memory, *Physica A*, **515** (2019), 440–449. https://doi.org/10.1016/j.physa.2018.09.171
15. R. Sipahi, F. M. Atay, S. I. Niculescu, Stability of traffic flow behavior with distributed delays modeling the memory effects of the drivers, *SIAM J. Appl. Math.*, **68** (2008), 738–759. https://doi.org/10.1137/060673813
16. Y. Chang, Z. He, R. Cheng, An extended lattice hydrodynamic model considering the driver's sensory memory and delayed-feedback control, *Physica A*, **514** (2008), 522–532. https://doi.org/10.1016/j.physa.2018.09.097
17. Y. Sun, H. Ge, R. Cheng, An extended car-following model considering driver's memory and average speed of preceding vehicles with control strategy, *Physica A*, **521** (2019), 752–761. https://doi.org/10.1016/j.physa.2019.01.092
18. Z. Xin, J. Xu, Analysis of a car-following model with driver memory effect, *Int. J. Bifurcation Chaos*, **25** (2015), 1550057. https://doi.org/10.1142/S0218127415500571
19. C. Zhai, W. Wu, A new continuum model with driver's continuous sensory memory and preceding vehicle's taillight, *Commun. Theor. Phys.*, **72** (2020), 105004.

20. M. Zhou, X. Qu, X. Li, A recurrent neural network based microscopic car following model to predict traffic oscillation, *Transp. Res. Part C Emerging Technol.*, **84** (2017), 245–264. https://doi.org/10.1016/j.trc.2017.08.027
21. X. Pei, Y. Pan, H. Wang, S. Wong, K. Choi, Empirical evidence and stability analysis of the linear car-following model with gamma-distributed memory effect, *Physica A*, **449** (2016), 311–323. https://doi.org/10.1016/j.physa.2015.12.104
22. R. Sipahi, F. M. Atay, S. I. Niculescu, Stability of traffic flow behavior with distributed delays modeling the memory effects of the drivers, *SIAM J. Appl. Math.*, **68** (2008), 738–759. https://doi.org/10.1137/060673813
23. M. A. Hossain, J. Tanimoto, The "backward-looking" effect in the continuum model considering a new backward equilibrium velocity function, *Nonlinear Dyn.*, **106** (2021), 2061–2072. https://doi.org/10.1007/s11071-021-06894-2
24. D. Jia, D. Ngoduy, Enhanced cooperative car-following traffic model with the combination of V2V and V2I communication, *Transp. Res. Part B Methodol.*, **90** (2016), 172–191. https://doi.org/10.1016/j.trb.2016.03.008
25. J. Xiao, M. Ma, S. Liang, G. Ma, The non-lane-discipline-based car-following model considering forward and backward vehicle information under connected environment, *Nonlinear Dyn.*, **107** (2022), 2787–2801. https://doi.org/10.1007/s11071-021-06999-8
26. D. Ngoduy, Analytical studies on the instabilities of heterogeneous intelligent traffic flow, *Commun. Nonlinear Sci. Numer. Simul.*, **18** (2013), 2699–2706. https://doi.org/10.1016/j.cnsns.2013.02.018
27. J. Larsson, M. F. Keskin, B. Peng, B. Kulcsár, H. Wymeersch, Pro-social control of connected automated vehicles in mixed-autonomy multi-lane highway traffic, *Commun. Transp. Res.*, **1** (2021), 100019. https://doi.org/10.1016/j.commtr.2021.100019
28. Y. Li, W. Chen, S. Peeta, Y. Wang, Platoon control of connected multi-vehicle systems under V2X communications: design and experiments, *IEEE Trans. Intell. Transp. Syst.*, **21** (2019), 1891–1902.
29. D. Ngoduy, Effect of the car-following combinations on the instability of heterogeneous traffic flow, *Transportmetrica B Transport Dyn.*, **3** (2015), 44–58. https://doi.org/10.1080/21680566.2014.960503
30. B. Wang, T. M. Adams, W. Jin, Q. Meng, The process of information propagation in a traffic stream with a general vehicle headway: A revisit, *Transp. Res. Part C Emerging Technol.*, **18** (2010), 367–375. https://doi.org/10.1016/j.trc.2009.05.011
31. X. Wang, Modeling the process of information relay through inter-vehicle communication, *Transp. Res. Part B Methodol.*, **41** (2007), 684–700. https://doi.org/10.1016/j.trb.2006.11.002
32. W. Jin, W. W. Recker, Instantaneous information propagation in a traffic stream through inter-vehicle communication, *Transp. Res. Part B Methodol.*, **40** (2006), 230–250. https://doi.org/10.1016/j.trb.2005.04.001
33. A. Kesting, M. Treiber, D. Helbing, Enhanced intelligent driver model to access the impact of driving strategies on traffic capacity, *Philos. Trans. R. Soc. A Math. Phys. Eng. Sci.*, **368** (2010), 4585–4605. https://doi.org/10.1098/rsta.2010.0084
34. Y. Li, L. Zhang, S. Peeta, X. He, T. Zheng, Y. Li, A car-following model considering the effect of electronic throttle opening angle under connected environment, *Nonlinear Dyn.*, **85** (2016), 2115–2125. https://doi.org/10.1007/s11071-016-2817-y

35. J. Wu, X. Qu, Intersection control with connected and automated vehicles: a review, *J. Intell. and Connected Veh.*, **5** (2022), 260–269. https://doi.org/10.1108/JICV-06-2022-0023
36. T. Olovsson, T. Svensson, J. Wu, Future connected vehicles: Communications demands, privacy and cyber-security, *Commun. Transp. Res.*, **2** (2022), 100056. https://doi.org/10.1016/j.commtr.2022.100056
37. K. L. Lim, J. Whitehead, D. Jia, Z. Zheng, State of data platforms for connected vehicles and infrastructures, *Commun. Transp. Res.*, **1** (2021), 10001. https://doi.org/10.1016/j.commtr.2021.100013
38. D. Ngoduy, S. Lee, M. Treiber, H. Vu, Langevin method for a continuous stochastic car-following model and its stability conditions, *Transp. Res. Part C Emerging Technol.*, **105** (2019), 599–610. https://doi.org/10.1016/j.trc.2019.06.005
39. R. Jiang, M. Hu, H. Zhang, Z. Gao, B. Jia, Q. Wu, et al., Traffic experiment reveals the nature of car-following, *PloS One.*, **9** (2014), 94351. https://doi.org/10.1371/journal.pone.0094351
40. R. Jiang, M. Hu, H. Zhang, Z. Gao, B. Jia, Q. Wu, On some experimental features of car-following behavior and how to model them, *Transp. Res. Part B Methodol.*, **80** (2015), 338–354. https://doi.org/10.1016/j.trb.2015.08.003
41. R. Jiang, C. Jin, H. Zhang, Y. Huang, J. Tian, W. Wang, et al., Experimental and empirical investigations of traffic flow instability, *Transp. Res. Part C Emerging Technol.*, **94** (2018), 83–98. https://doi.org/10.1016/j.trc.2017.08.024
42. J. Tian, R. Jiang, B. Jia, Z. Gao, S. Ma, Empirical analysis and simulation of the concave growth pattern of traffic oscillations, *Transp. Res. Part B Methodol.*, **93** (2016), 338–354. https://doi.org/10.1016/j.trb.2016. 08.001
43. J. Tian, H. Zhang, M. Treiber, R. Jiang, Z. Gao, B. Jia, On the role of speed adaptation and spacing indifference in traffic instability: Evidence from car-following experiments and its stochastic model, *Transp. Res. Part B Methodol.*, **129** (2019), 334–350. https://doi.org/10.1016/j.trb.2019.09.014
44. F. Zheng, S. E. Jabari, H. Liu, D. Liu, Traffic state estimation using stochastic Lagrangian dynamics, *Transp. Res. Part B Methodol.*, **115** (2018), 143–165. https://doi.org/10.1016/j.trb.2018.07.004
45. J. A. Laval, C. S. Toth, Y. Zhou, A parsimonious model for the formation of oscillations in car-following models, *Transp. Res. Part B Methodol.*, **70** (2014), 228–238. https://doi.org/10.1016/j.trb.2014.09.004
46. K. Yuan, J. Laval, V. L. Knoop, R. Jiang, S. P. Hoogendoorn, A geometric Brownian motion car-following model: towards a better understanding of capacity drop, *Transportmetrica B Transport Dyn.*, **21** (2018), 915–927. https://doi.org/10.1080/21680566.2018.1518169
47. J. Tian, C. Zhu, D. Chen, R. Jiang, G. Wang, Z. Gao, Car following behavioral stochasticity analysis and modeling: Perspective from wave travel time, *Transp. Res. Part B Methodol.*, **143** (2021), 160–176. https://doi.org/10.1016/j.trb.2020.11.008
48. D. Ngoduy, Noise-induced instability of a class of stochastic higher order continuum traffic models, *Transp. Res. Part B Methodol.*, **150** (2021), 260–278. https://doi.org/10.1016/j.trb.2021.06.013

49. P. Lin, X. Liu, M. Pei, P. Wu, Revealing the spatial variation in vehicle travel time with weather and driver travel frequency impacts: Findings from the Guangdong-Hong Kong-Macao Greater Bay Area, China, *Electron. Res. Arch.*, **30** (2022), 3711–3734. https://doi.org/10.3934/era.2022190
50. P. Wagner, A time-discrete harmonic oscillator model of human car-following, *Eur. Phys. J. B*, **84** (2011), 713–718. https://doi.org/10.1140/epjb/e2011-20722-8
51. P. Wagner, Analyzing fluctuations in car-following, *Transp. Res. Part B Methodol.*, **46** (2012), 1384–1392. https://doi.org/10.1016/j.trb.2012.06.007
52. M. Makridis, L. Leclercq, B. Ciuffo, G. Fontaras, K. Mattas, Formalizing the heterogeneity of the vehicle-driver system to reproduce traffic oscillations, *Transp. Res. Part C Emerging Technol.*, **120** (2020), 102803. https://doi.org/10.1016/j.trc.2020.102803
53. J. Wen, C. Wu, R. Zhang, X. Xiao, N. Nv Y. Shi, Rear-end collision warning of connected automated vehicles based on a novel stochastic local multivehicle optimal velocity model, *Accid. Anal. Prev.*, **148** (2020), 105800. https://doi.org/10.1016/j.aap.2020.105800
54. X. Mao, *Stochastic Differential Equations and Applications*, Horwood, Chichester, 2008.
55. R. Ortega, Variations on Lyapunov's stability criterion and periodic prey-predator systems, *Electron. Res. Arch.*, **29** (2021), 3995. https://doi.org/10.3934/era.2021069

Appendix A. Stability condition derivation for S-SFVDM

Expand $\delta v_n(t) = \zeta_1 e^{in\omega+zt}$ and $\delta x_n(t) = \zeta_2 e^{in\omega+zt}$. ζ_1 and ζ_2 are constants. Therefore, Equation (34) can be read as the linear stochastic ordinary differential equation:

$$d\mathrm{X}(t) = \mathrm{P_{SG}X}(t)dt + \mathrm{Q_{SG}X}(t)dW(t) \tag{A1}$$

where

$$\mathrm{P_{SG}} = \begin{bmatrix} 0 & e^{-i\omega}-1 \\ \alpha V' & -\alpha + \lambda\left(e^{-i\omega}-1\right) + \rho(\lambda,k,\tau,\eta,\phi) \end{bmatrix} \tag{A2}$$

$$\mathrm{Q_{SG}} = \begin{bmatrix} 0 & 0 \\ \alpha\sigma\beta & 0 \end{bmatrix} \tag{A3}$$

$$\rho(k,\tau,\eta,\varphi) = \phi\tau\eta\sum_{k=0}^{Ts} f_\Gamma(k\tau)e^{-zk\tau} + \phi\tau(1-\eta)\sum_{k=0}^{Ts} f_\Gamma(k\tau)e^{-i\omega-zk\tau} \tag{A4}$$

Based on Definition 1, **Theorem 3** and the corresponding proof will be derived.

Theorem 3. The stochastic car-following model with the speed guidance strategy considered is 2nd-moment exponentially stable if

$$\sigma^2 < \frac{4\left(\alpha+\lambda+\phi\eta\tau\sum_{k=0}^{Ts} f_\Gamma(k\tau) - \sqrt{\left[\lambda-\phi(1-\eta)\tau\sum_{k=0}^{Ts} f_\Gamma(k\tau)\right]^2 + 2\left(1-\phi\tau^2\sum_{k=0}^{Ts} k f_\Gamma(k\tau)\right)\alpha V_{op}'}\right)}{\alpha^2\beta^2} \tag{A5}$$

where $Ts = T/\tau$.

Proof. The characteristic equation of the matrix P is

$$z^2 - z\left(-\alpha + \lambda\left(e^{-iw} - 1\right) + \phi\tau\left[\eta\sum_{k=0}^{Ts} f_\Gamma(k\tau)e^{-\lambda i\tau} + (1-\eta)\sum_{k=0}^{Ts} f_\Gamma(k\tau)e^{-i\omega-\lambda k\tau}\right]\right) -$$

$$\alpha V'\left(e^{-i\omega} - 1\right) = 0 \tag{A6}$$

Expanding $z = i\omega z_1 + \omega^2 z_2 + \cdots$ into Eq (A6) and ignoring the high-order terms by setting the first-order and second-order terms to zeros, the expressions of z_1 and z_2 can be obtained:

$$z_1 = \frac{-\alpha V'}{\alpha+\phi\tau\sum_{k=0}^{Ts} f_\Gamma(k\tau)-\frac{1}{2}\alpha^2\beta^2\sigma^2} \tag{A7}$$

$$\frac{\left(1-\phi\tau^2\sum_{k=0}^{Ts} k f_\Gamma(k\tau)\right)\left(\frac{\alpha V'}{\alpha+\phi\tau\sum_{k=0}^{Ts} f_\Gamma(k\tau)-\frac{1}{2}\alpha^2\beta^2\sigma^2}\right)^2+\left[\lambda-\phi(1-\eta)\tau\sum_{k=0}^{Ts} f_\Gamma(k\tau)\right]\left(\frac{-\alpha V'}{\alpha+\phi\tau\sum_{k=0}^{Ts} f_\Gamma(k\tau)-\frac{1}{2}\alpha^2\beta^2\sigma^2}\right)+\frac{1}{2}\alpha V'}{\alpha+\phi\tau\sum_{k=0}^{Ts} f_\Gamma(k\tau)-\frac{1}{2}\alpha^2\beta^2\sigma^2} \tag{A8}$$

The condition of stochastic stability will be held only if $z_1 < 0$ and $z_2 < 0$. Therefore, we can obtain the stability conditions by taking σ as the variable:

$$\sigma^2 < \frac{4\left(\alpha+\lambda-\phi\eta\tau\sum_{k=0}^{Ts} f_\Gamma(k\tau)-\sqrt{\left[\lambda-\phi(1-\eta)\tau\sum_{k=0}^{Ts} f_\Gamma(k\tau)\right]^2+2\left(1-\phi\tau^2\sum_{k=0}^{Ts} k f_\Gamma(k\tau)\right)\alpha V_{op}{}'}\right)}{\alpha^2\beta^2} \tag{A9}$$

When $\tau\sum_{k=0}^{Ts} f_\Gamma(k\tau) \approx 1$ (for example, $Ts > 100 = 10s$ and $\tau\sum_{k=0}^{Ts} f_\Gamma(k\tau) \approx 1$ for $u = 2$ and $m = 1$; 10 s was deemed as a reasonable value of the length of effective memory time of drivers [18]), Equation (A9) can be simplified as

$$\sigma^2 < \frac{4\left(\alpha+\lambda-\phi\eta-\sqrt{[\lambda-\phi(1-\eta)]^2+2\left(1-\phi\tau^2\sum_{k=0}^{Ts} k f_\Gamma(k\tau)\right)\alpha V_{op}{}'}\right)}{\alpha^2\beta^2} \tag{A10}$$